https://doi.org/10.1016/j.apacoust.2018.01.015

Technical Note

Hybrid noise control in a duct using a periodic dual Helmholtz resonator array

Chenzhi Cai and Cheuk Ming Mak*

Department of Building Services Engineering, The Hong Kong Polytechnic University, Hung Hom, Kowloon, Hong Kong, China

chenzhi.cai@connect.polyu.hk, cheuk-ming.mak@polyu.edu.hk

*Corresponding author.
E-mail Address: cheuk-ming.mak@polyu.edu.hk (C.M.Mak).
Telephone: +852 2766 5856
Fax: +852 2765 7198

Abstract

This paper focuses on the hybrid noise control in a duct using a periodic dual Helmholtz resonator (HR) array. A dual HR which consists of two HRs connected in series (neck-cavity-neck-cavity) leads to two resonance frequencies. A dual HR is analogous to a two degrees of freedom mechanical system. Based on the lumped model, the resonance frequencies and transmission loss of a dual HR have been derived. However, a dual HR is only effective at its resonance peaks with relative narrow bands. Aiming at broader noise attenuation bands for hybrid noise control at low frequencies, a periodic dual HR array is proposed in this paper. The wave propagation in a duct mounted with a periodic dual HR array is investigated theoretically and numerically. The Bragg wave theory and transfer matrix method are developed to conduct the investigation. The predicted theoretical results fit well with the Finite Element Method. Owing to the coupling of Bragg reflection and dual HR's resonances, a periodic dual array can provide much broader noise attenuation bands at the designed resonance frequencies of the dual HR. The proposed periodic dual HR array can be used in practical engineering work to reduce hybrid noise at low frequencies.

Keywords: hybrid noise control; dual Helmholtz resonator; periodic; transmission loss

1. Introduction

Ductwork systems have wide applications in engineering, such as ventilation and air conditioning system in buildings, aircraft jet engines, automotive air ducts and hydraulic system [1-3]. The components of the ductwork system, for instance, dampers, bends transition pieces, corners or even attenuators punctuate the original uniform ductwork, which are responsible for the generation of the undesired noise as the ductwork system begins to work [4]. Abatement of ductwork noise has always been a challenge, especially the low-frequency and broadband noise in a ventilation ductwork system due to its significant role in modern buildings to maintain good indoor environment [5]. The accompanied duct noise from the ventilation system could propagate into the occupied zones through the waveguide and could deteriorate human being's working or living environment quality [6,7]. Therefore, it is not surprising that noise attenuation technologies for the ventilation ductwork system have received extensive attentions.

Most traditional methods such as dissipative silencer and passive reactive silencer still suffer from some serious drawbacks despite these silencers are widely used in ventilation ductwork system. The dissipative silencer performances well at mid to high frequencies, however, it fails to be effective at low frequencies because of its high characteristics impedance [8,9]. Meanwhile accumulation of dusts and bacterial breeding in porous sound absorption materials are notable environmental issues. Passive reactive silencers, the Helmholtz resonator (hereafter HR) and expansion chamber are typical examples, show stable noise attenuation performance and can be tuned conveniently. Nevertheless, the volume of the expansion chamber needs to be sufficiently large in order to deal with low frequencies noise [10]. The presence of HR offers a solution of low-frequency noise control,

yet it qualifies as a narrow band noise attenuator that it is only effective at its resonance with a relative narrow frequency range [11-13].

The narrow-band behavior of a HR at its single resonance peak makes it not suitable in engineering applications and is unable to deal with hybrid noise. In order to mitigate multiple tones, HR with a variety of modifications have been proposed. Griffin et al. [14] demonstrated a parallel-coupled HR through a thin membrane to obtain three resonance frequencies instead of two. Xu et al. [15] proposed a dual HR formed a pair of neck and cavity connected in series and illustrated that a dual HR can lead to two resonances at low frequencies. Guan and Jiao [16] analyzed a three degrees of freedom HR which consists of three necks and cavities and proposed an optimal design method to inspect the unknown size parameter values for resonance frequencies coinciding with the input fundamental frequencies. Park [17] investigated the acoustic properties of micro-perforated panel absorbers backed by Helmholtz resonators for the improvement of low-frequency noise reduction. Besides these endeavors to modified HRs, some researchers aim at a broader noise attenuation band at low frequencies. An array of HRs is one possible way to carry out this objective. Bradly [18,19] analyzed the propagation of time harmonic acoustic wave in periodic waveguides theoretically and experimentally. Sugimoto and Horioka [20] investigated the peculiar dispersion characteristics of sound waves propagation in a tunnel with an array of identical HRs mounted periodically, marked as stopbands and passbands. Cai and Mak [21,22] proposed a noise control zone compromising the attenuation bandwidth or peak amplitude of a periodic ducted HR system, and improved the noise attenuation performance of the system by adding HRs. Owing to the coupling of Bragg reflection and HR's resonance, a periodic HR array can provide a much broader noise

attenuation bands at the HR's resonance frequency. However, it cannot deal with the hybrid noise which often occurs in practical engineering.

The mechanism of Bragg reflection and modified HRs motivate us to achieve several broadband noise attenuation bands in low-frequency range. This paper focuses on the hybrid noise control by using a periodic ducted dual HR system. The dual HR which consists of two HRs connected in series (neck-cavity-neck-cavity) leads to two resonance frequencies. The geometries of the dual HR are significant small compared with the wavelength of oscillation. Hence, the lumped parameter theory is employed to approximate the dual HR as an equivalent two degrees of freedom mechanical system. An array of dual HRs is mounted on the duct periodically. In the interest of low frequencies, the frequency range considered in this paper is well below the duct's cutoff frequency. It is therefore that only planar wave is allowed to propagate in the duct. The Bragg wave theory and transfer matrix method are developed to conduct the investigation. The theoretical predictions are validated by Finite Element Method (FEM) simulation.

2. Theoretical model of a dual Helmholtz resonator

A dual HR formed by two HRs connected in series (neck-cavity-neck-cavity) leads to two resonance frequencies. A dual HR could be analogous to a two degrees of freedom mechanical system, as illustrated in Fig. 1. The mass of air in the first neck, which is communicating with the duct, is driven by an external force and two cavities are regarded as spring. According to Hooke's law, it should be noted that the first string has different stiffness (K_{11} and K_{12}) to the front and rear masses connected on it. By applying the Newton's second law of motion to the first mass M_1 and the second M_2 respectively yield:

$$M_1\frac{d^2x_1}{dt^2}+R_1\frac{dx_1}{dt}+K_{11}x_1=S_1p_0e^{j\omega t},\ M_2\frac{d^2x_2}{dt^2}+R_2\frac{dx_2}{dt}+K_{22}x_2=K_{12}x_2 \tag{1}$$

where $M_1=\rho_0S_1l_{n1}'$ and $M_2=\rho_0S_2l_{n2}'$ are the corresponding mass of air in the necks including the end-correction factor (ρ_0 is air density, l_{n1}' and l_{n2}' are necks' effective length including the end-correction factor, S_1 and S_2 are necks' area), R_1 and R_2 are damping coefficients of necks, K_{11} and K_{12} represent the stiffness of the first spring to the first mass and second mass respectively, $K_2=\rho_0c_0^2S_2{}^2/V_2$ (V_i with subscript $i=1,2$ represent the first and second cavity volume respectively, c_0 is the speed of sound in the air) is the stiffness of the second spring, $e^{j\omega t}$ is the time-harmonic disturbance. Applying the Hooke's law to the mechanical analogy of a dual HR, the stiffness K_{11} and K_{12} could be obtained as:

$$K_{11}=\frac{\rho_0c_0^2S_1}{V_1x_1}(S_1x_1-S_2x_2),\qquad K_{12}=\frac{\rho_0c_0^2S_2}{V_1x_2}(S_1x_1-S_2x_2) \tag{2}$$

By introducing Eq. (2) into Eq. (1) yields:

$$\begin{cases} M_1\dfrac{d^2x_1}{dt^2}+R_1\dfrac{dx_1}{dt}+\dfrac{\rho_0c_0^2S_1}{V_1}(S_1x_1-S_2x_2)=S_1p_0e^{j\omega t} \\ M_2\dfrac{d^2x_2}{dt^2}+R_2\dfrac{dx_2}{dt}+\dfrac{\rho_0c_0^2S_2^2}{V_1}x_2-\dfrac{\rho_0c_0^2S_2}{V_1}(S_1x_1-S_2x_2)=0 \end{cases} \tag{3}$$

Substituting $x_1=X_1e^{j\omega t}$ and $x_2=X_2e^{j\omega t}$ into Eq. (3) and rearranging in the matrix form as:

$$\begin{bmatrix} -\omega^2M_1+j\omega R_1+\dfrac{\rho_0c_0^2S_1^2}{V_1} & -\dfrac{\rho_0c_0^2S_1S_2}{V_1} \\ -\dfrac{\rho_0c_0^2S_1S_2}{V_1} & -\omega^2M_2+j\omega R_2+\rho_0c_0^2S_2^2\dfrac{(V_1+V_2)}{V_1V_2} \end{bmatrix}\begin{Bmatrix} X_1e^{j\omega t} \\ X_2e^{j\omega t} \end{Bmatrix}=\begin{Bmatrix} S_1p_0e^{j\omega t} \\ 0 \end{Bmatrix} \tag{4}$$

where X_1 and X_2 are the magnitudes of the first and the second neck's displacement respectively. Eq. (4) could be simplified as:

$$\begin{bmatrix} a_{11} & a_{12} \\ a_{21} & a_{22} \end{bmatrix} \begin{Bmatrix} X_1 \\ X_2 \end{Bmatrix} = \begin{Bmatrix} p_0 S_1 \\ 0 \end{Bmatrix} \tag{5}$$

where $\begin{bmatrix} -\omega^2 M_1 + j\omega R_1 + \dfrac{\rho_0 c_0^2 S_1^2}{V_1} & -\dfrac{\rho_0 c_0^2 S_1 S_2}{V_1} \\ -\dfrac{\rho_0 c_0^2 S_1 S_2}{V_1} & -\omega^2 M_2 + j\omega R_2 + \rho_0 c_0^2 S_2^2 \dfrac{(V_1 + V_2)}{V_1 V_2} \end{bmatrix} = \begin{bmatrix} a_{11} & a_{12} \\ a_{21} & a_{22} \end{bmatrix}$.

According to Eq. (5), the relation of X_1 and $p_0 S_1$ could be described as $X_1 = p_0 S_1 a_{22} / (a_{11} a_{22} - a_{12} a_{21})$. It is therefore that the acoustic impedance of the dual HR could be obtained as:

$$Z_r = \frac{p_0}{j\omega X_1 S_1} = \frac{1}{j\omega {S_1}^2} \frac{a_{11} a_{22} - a_{12} a_{21}}{a_{22}} \tag{6}$$

By ignored the effect of viscous dissipation through the necks for simplicity ($R_1 = R_2 = 0$), Eq.(6) could be rewritten as:

$$Z_r = \frac{1}{j\omega {S_1}^2} \frac{M_1 M_2 \omega^4 - \rho_0 c_0^2 [M_1 S_2^2 (\frac{1}{V_1} + \frac{1}{V_2}) + M_2 S_1^2 \frac{1}{V_1}] \omega^2 + \frac{{\rho_0}^2 c_0^4 {S_1}^2 {S_2}^2}{V_1 V_2}}{\rho_0 c_0^2 S_2^2 (\frac{1}{V_1} + \frac{1}{V_2}) - M_2 \omega^2} \tag{7}$$

It is therefore that the dual HR's angular resonance frequencies are the roots of the following equation:

$$M_1 M_2 \omega^4 - \rho_0 c_0^2 [M_1 S_2^2 (\frac{1}{V_1} + \frac{1}{V_2}) + M_2 S_1^2 \frac{1}{V_1}] \omega^2 + \frac{{\rho_0}^2 c_0^4 {S_1}^2 {S_2}^2}{V_1 V_2} = 0 \tag{8}$$

Then, the resonance frequencies of the dual HR can be derived from Eq. (8) and be expressed as:

$$f_{1,2}=\frac{1}{2\pi}\sqrt{\frac{\rho_0 c_0^2}{2}\left(\frac{S_2^2}{V_1M_2}+\frac{S_2^2}{V_2M_2}+\frac{S_1^2}{V_1M_1}\right)\mp\sqrt{\frac{\rho_0{}^2c_0^4}{4}\left(\frac{S_2^2}{V_1M_2}+\frac{S_2^2}{V_2M_2}+\frac{S_1^2}{V_1M_1}\right)^2-\frac{\rho_0{}^2c_0^4S_1{}^2S_2{}^2}{M_1M_2V_1V_2}}} \tag{9}$$

It can be observed from Eq. (9) that the resonance frequencies of the dual HR are only determined by its geometries. Therefore, it is straightforward to design a dual HR with desired resonance frequencies. Once the acoustic impedance is obtained, the transmission loss of the side-branch dual HR mounted on the duct with cross-sectional area S_d could be given as [2]:

$$TL=20\log_{10}\left(\frac{1}{2}\left|2+\frac{\rho_0 c_0}{S_d}\frac{1}{Z_r}\right|\right) \tag{10}$$

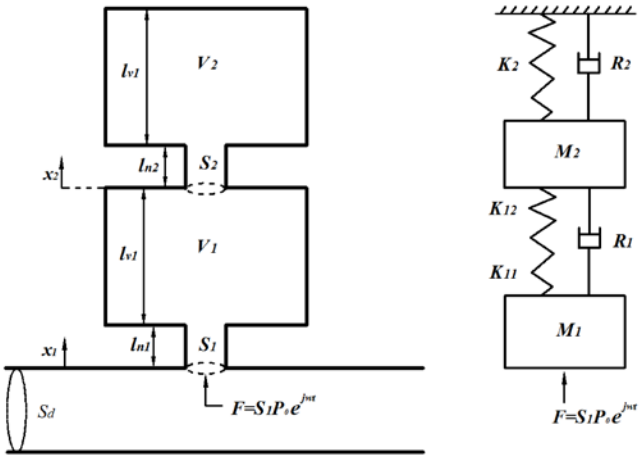

Fig. 1 Mechanical analogy of a dual Helmholtz resonator

3. Wave propagation in a duct with a periodic dual Helmholtz resonator array

A periodic structure that consists of a number of identical structure components distributed periodically. Wave propagation in a periodic system is known as Bloch wave

[18]. Only planar wave is considered in duct propagation because the low frequencies of interest are well below the duct's cutoff frequency. Bloch wave theory and transfer matrix method are used to investigate the acoustic performance of the periodic dual HR system.

3.1 Bloch wave in the periodic dual Helmholtz resonator system

The periodic dual HR system, consisting of a uniform duct with dual HRs attached periodically, is demonstrated in Fig. 2. A duct segment with a side-branch dual HR is considered as a typical periodic unit. The diameter of the dual HR's neck is inappreciable compared with the length of the duct segment in a periodic unit. Therefore, the length of the duct segment is regarded as the periodic distance. The sound properties in the *nth* cell could be described as sound pressure $p_n(x)$ and particle velocity $u_n(x)$. In light of the low frequencies of interest in the present study, only planar wave is assumed to propagate through the duct. The sound pressure is a combination of positive-*x* and negative-*x* directions. Assuming a time-harmonic disturbance in the form of $e^{j\omega t}$, the sound pressure and particle velocity are expressed as:

$$p_n(x) = I_n e^{-jk(x-x_n-\omega t)} + R_n e^{jk(x-x_n+\omega t)} \tag{11}$$

$$u_n(x) = \frac{I_n}{S_d Z_d} e^{-jk(x-x_n-\omega t)} - \frac{R_n}{S_d Z_d} e^{jk(x-x_n+\omega t)} \tag{12}$$

where k is the number of waves, $x_n = (n-1)d$ represents the local coordinates, d is the periodic distance, S_d is the cross-sectional area of the duct, Z_d is the acoustic impedance of the duct, and I_n and R_n represent respective complex wave amplitudes. By introducing the continuity conditions of the sound pressure and volume velocity at the duct-neck interface that at $x = nd$, Eq. (11) and Eq. (12) may be seen to readily yield the following transfer matrix:

$$\begin{bmatrix} I_{n+1} \\ R_{n+1} \end{bmatrix} = \begin{bmatrix} (1-\frac{Z_d}{2Z_r})\exp(-jkd) & -\frac{Z_d}{2Z_r}\exp(jkd) \\ \frac{Z_d}{2Z_r}\exp(-jkd) & (1+\frac{Z_d}{2Z_r})\exp(jkd) \end{bmatrix} \begin{bmatrix} I_n \\ R_n \end{bmatrix} = \mathbf{T} \begin{bmatrix} I_n \\ R_n \end{bmatrix} \tag{13}$$

$\mathbf{T}$ is the transfer matrix. The sound pressure and particle velocity in an arbitrary can be obtained successively by Eq. (13) once the initial sound pressure is known. According to Bloch wave theory [18], Eq. (13) can be described as:

$$\begin{bmatrix} I_{n+1} \\ R_{n+1} \end{bmatrix} = \lambda \begin{bmatrix} I_n \\ R_n \end{bmatrix} = \mathbf{T} \begin{bmatrix} I_n \\ R_n \end{bmatrix} \tag{14}$$

where λ is set to be $\exp(-jqd)$, and q is the Bloch wave number and is allowed to be a complex value. Then, the analysis of the periodic structure boils down to the solution of eigenvalues and corresponding eigenvectors problem. There are two eigenvalue solutions of λ: λ_1 and λ_2 with corresponding eigenvectors $[v_{I1}, v_{R1}]^{\mathrm{T}}$ and $[v_{I2}, v_{R2}]^{\mathrm{T}}$ respectively. Then, Eq. (14) can be rewritten in eigenvector form as:

$$\begin{bmatrix} I_{n+1} \\ R_{n+1} \end{bmatrix} = \mathbf{T} \begin{bmatrix} I_n \\ R_n \end{bmatrix} = \mathbf{T}^2 \begin{bmatrix} I_{n-1} \\ R_{n-1} \end{bmatrix} = \ldots = \mathbf{T}^n \begin{bmatrix} I_1 \\ R_1 \end{bmatrix} = A_0 \lambda_1^n \begin{bmatrix} v_{I1} \\ v_{R1} \end{bmatrix} + B_0 \lambda_2^n \begin{bmatrix} v_{I2} \\ v_{R2} \end{bmatrix} \tag{15}$$

where A_0 and B_0 are complex constants and can be solved with the boundary conditions. The incident wave in the initial part is I_0 and the transmitted wave in the last part is I_{n+1}. The average transmission loss of each HR of the whole system can be expressed as:

$$\overline{TL} = \frac{20}{n+1}\log_{10}\left|\frac{I_0}{I_{n+1}}\right| = \frac{20}{n+1}\log_{10}\left|\frac{A_0\lambda_1^{-1}v_{I1} + B_0\lambda_2^{-1}v_{I2}}{A_0\lambda_1^{n-1}v_{I1} + B_0\lambda_2^{n-1}v_{I2}}\right| \tag{16}$$

The duct is assumed to end up with an anechoic termination. It means that there is no reflection in the last part. Therefore, B_0 is required to be zero. Eq. (16) can be simplified

as: $\overline{TL} = -20\log_{10}|\lambda_1|$ for the average transmission loss of a duct with an anechoic termination loaded with dual HRs periodically.

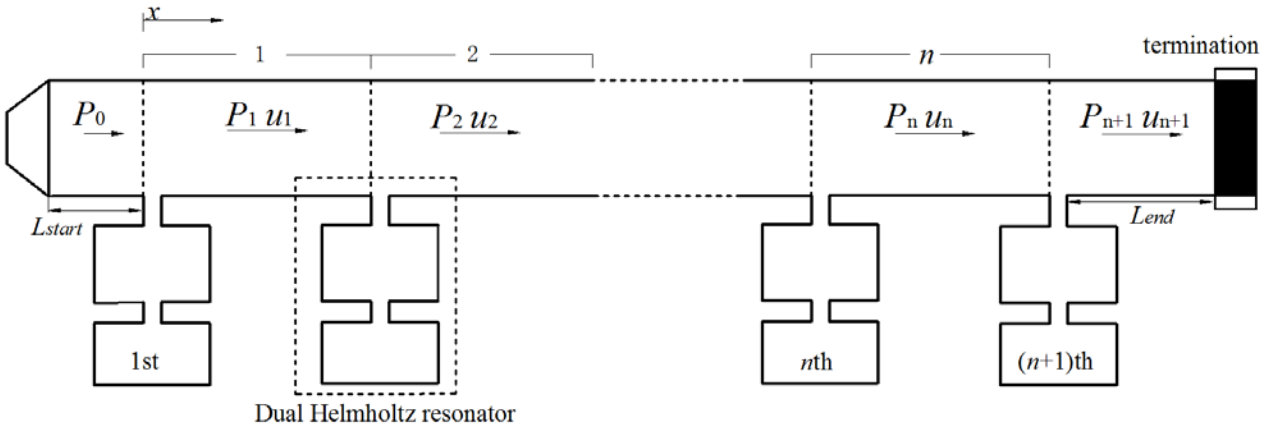

Fig. 2 Schematic diagram of a periodic dual HR system

3.2 Coupling of Bragg reflection and dual HR's resonances

The transmission loss of the periodic dual HR system is only related to the solution of λ, as discussed above. Owing to the relation of q and λ, the transmission loss of the acoustic system refers to the solution of q. The solution of q, as a function of the wave frequencies, periodic distance and geometries of a duct resonator system, is allowed to be a complex. The real part and imaginary part of q are critical to distinguish the stopbands from passbands. The real part of q is referred to as passbands that have only a phase delay during wave propagation, and the imaginary part as attenuation constant named stopbands (decay of a wave happens from one unit to the following). It can be known that wave attenuation occurs for frequencies that provides an imaginary part to q. There are two mechanisms of the stopbands: dual HR's resonances and Bragg reflection. The stopbands caused by dual HR's resonances are situated near dual HR's resonance frequencies f_{01} and f_{02}, which is also the mechanism of a single dual HR case. The other kind of stopbands is

brought about physically by Bragg reflection and will exist near $f_m = mc_0 / 2d$ (m is an integer). The width of the stopband decrease as $1/m^2$ and the maximum value of the imaginary part becomes smaller as $1/m$ [20].

For a general HR with single resonance frequency, the periodic distance is chosen to be half-wavelength of HR's resonance frequency for the sake of the coupling of first Bragg reflection and HR's resonance. The dual HR has two resonance frequencies f_{01} and f_{02} (assuming $f_{01} < f_{02}$). In order to obtain broader noise attenuation bands at these two resonance frequencies, both the resonance frequencies are designed to coincide with Bragg reflection. Note that the Bragg reflection is exiting at $f_m = mc_0 / 2d$ (m is an integer). It is therefore that the resonance frequencies of the dual HR should also satisfy the relation of $f_{02} = mf_{01}$ for broader noise attenuation bands at the designed resonance frequencies. The resonance frequencies of a dual HR could be tuned straightforward due to they are only determined by its geometries. Once a dual HR's resonance frequencies are designed to be $f_{02} = 2f_{01}$, the periodic distance could be set as $d = \lambda_{01}/2 = \lambda_{02}$ (λ_{01} and λ_{02} are wavelength of f_{01} and f_{02} respectively) to make the first and second Bragg reflection coincide with two resonance frequencies of the dual HR respectively for the sake of broader noise attenuation bands.

4. Results and discussion

4.1 Validation of the theoretical prediction of a side-branch dual HR

The dual HR which consists of two HRs connected in series (neck-cavity-neck-cavity), as demonstrated in Fig. 1, leads to tow resonance frequencies. The resonance frequencies of a dual HR are only determined by its geometries. The geometries of the dual HR used

in this paper are: neck areas $S_1 = 0.25\pi$ cm^2 and $S_2 = 0.25\pi$ cm^2, neck lengths $l_{n1} = 2.5$ cm and $l_{n2} = 2.1$ cm, cavity volumes $V_1 = 115.2\pi$ cm^3 and $V_2 = 62.4\pi$ cm^3. The cross-sectional area of the main duct is $S_d = 25$ cm^2. Thus the resonance frequencies of the dual HR are 301 Hz and 602 Hz, which are calculated directly by Eq. (9). The three-dimensional FEM simulation using commercial software (COMSOL Multiphysics [23]) is adopted to verify the theoretical predictions. To ensure the accuracy, a fine mesh spacing of no more than 1/6 of the minimum wavelength of oscillation is adopted to divide the system into triangular elements. The predicted resonance frequencies fit well with the FEM simulation results, as illustrated in Fig. 3. The comparison of the transmission loss between the theoretical predictions and FEM simulation results for the side-branch dual HR are also exhibited in Fig. 3. The solid line represents the theoretical predictions, and the dashed line represents the FEM simulation results. A good agreement between the theoretical predictions and FEM simulations results can be observed in Fig. 3.

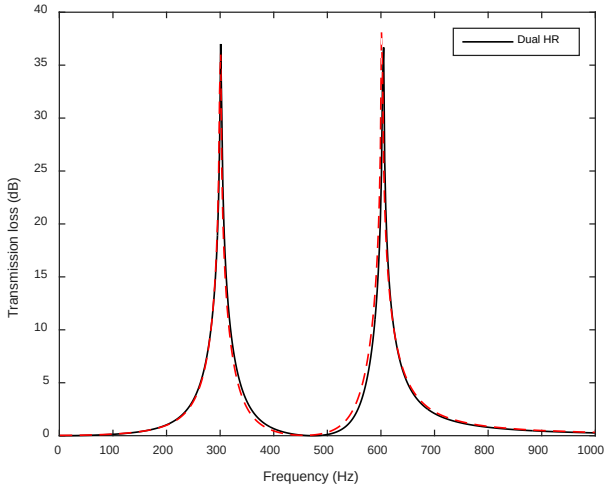

Fig. 3 Comparison of the theoretical predictions and FEM simulation results (solid line represents the theoretical predictions, and dashed line represents the FEM simulation results)

4.2 Validation of the predicted transmission loss of the periodic ducted HR system

The geometries of the dual HR and the main duct used here are the same as given above. The periodic dual HR system with an anechoic termination to avoid reflected waves from downstream is exhibited in Fig. 2. An oscillation sound pressure at a magnitude of $P_0 = 1$ is applied at the beginning of the duct as the initial boundary conditions. Fig. 4 shows the configuration of the periodic dual HR system consisting of six identical dual HRs mounted on the duct periodically. The average transmission loss ($\overline{TL}$) of a periodic dual HR array system is expressed as $\overline{TL} = -20\log_{10}|\lambda_1|$, which is only related to the solution of q. For the certain dual HR and main duct used in this paper, it indicates that the shape of $\overline{TL}$ is depended on the periodic distance. When the periodic distance is chosen to be $d = 0.58\lambda_{01}/2$, it can be observed from Fig. 5 that the dual HR's resonances and Bragg reflection have separated effects on the noise attenuation bands. The stopbands caused by resonance are situated near dual HR's resonance frequencies, and are the mechanism of a single dual HR case.

In order to obtain broader noise attenuation bands at designed resonance frequencies of the dual HR, the Bragg reflection is intended to coincide with resonance frequencies. The resonance frequencies of the dual HR are 301 Hz and 602 Hz, which is designed to satisfy the relation of $\lambda_{01} = 2\lambda_{02}$. Once the periodic distance is chosen to be $d = m\lambda_{01}/2$ (m is an integer), broader noise attenuation bands could be achieved at both resonance frequencies due to the coupling effect of Bragg reflection and dual HR's resonances, as

illustrated in Fig. 6. It can be seen from Fig. 6 that the width of noise attenuation bands at resonance frequencies decrease with the increasing of m. It is because of the stopbands brought by Bragg reflection decrease as $1/m^2$ in width. For the sake of broader noise attenuation bands at designed resonance frequencies of the dual HR, the periodic distance is chosen to be $d = \lambda_{01}/2 = \lambda_{02}$. Therefore, the first and second Bragg reflection can coincide with two resonance frequencies of the dual HR respectively. Fig. 7 compares noise attenuation bands of different periodic distance cases ($d = 0.5\lambda_{01}$ and $d = 0.58\lambda_{01}$) with or without considering coupling effects. The coupling of Bragg reflection and dual HR's resonances results in much broader noise attenuation bands at resonance frequencies of the dual HR. The FEM simulation used here is similar to the aforementioned description. The comparisons of the theoretical predicted results and the FEM simulation results with respect to different periodic distances are illustrated in Fig. 8, and the theoretical predictions fit well with the FEM simulation results.

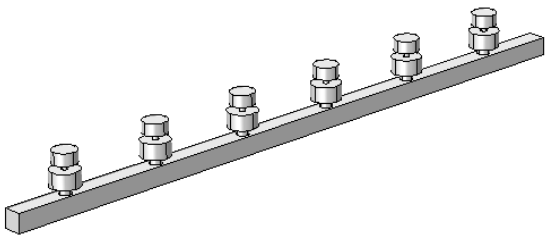

Fig. 4 Configuration of the periodic dual HR system consisting of six dual HRs

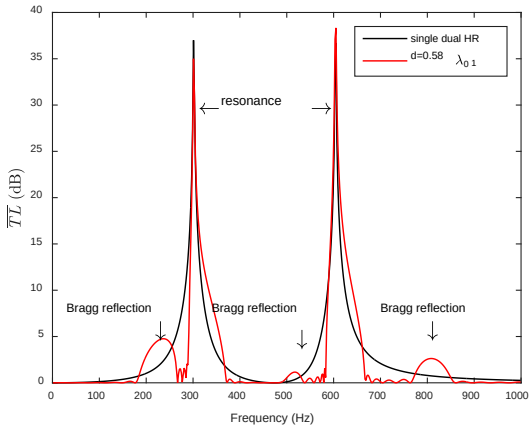

Fig. 5 Noise attenuation bands of the periodic dual HR system due to Bragg reflection and dual HR's resonances separately

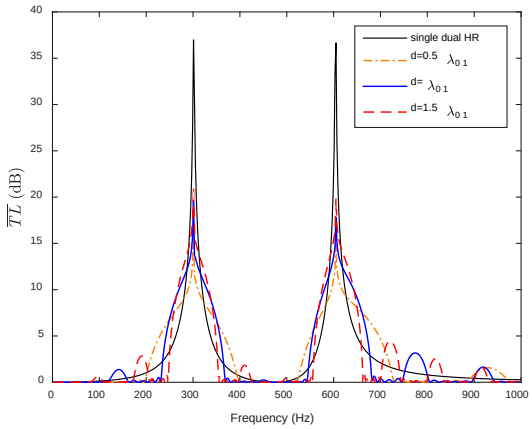

Fig. 6 Noise attenuation bands of the periodic dual HR system due to the coupling of Bragg reflection and dual HR's resonances

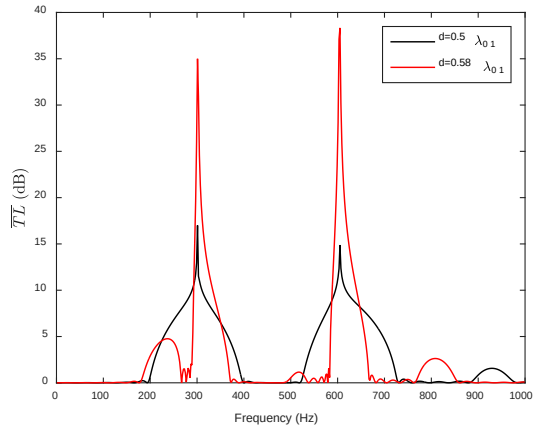

Fig. 7 Noise attenuation bands of the periodic dual array system with and without coupling effects

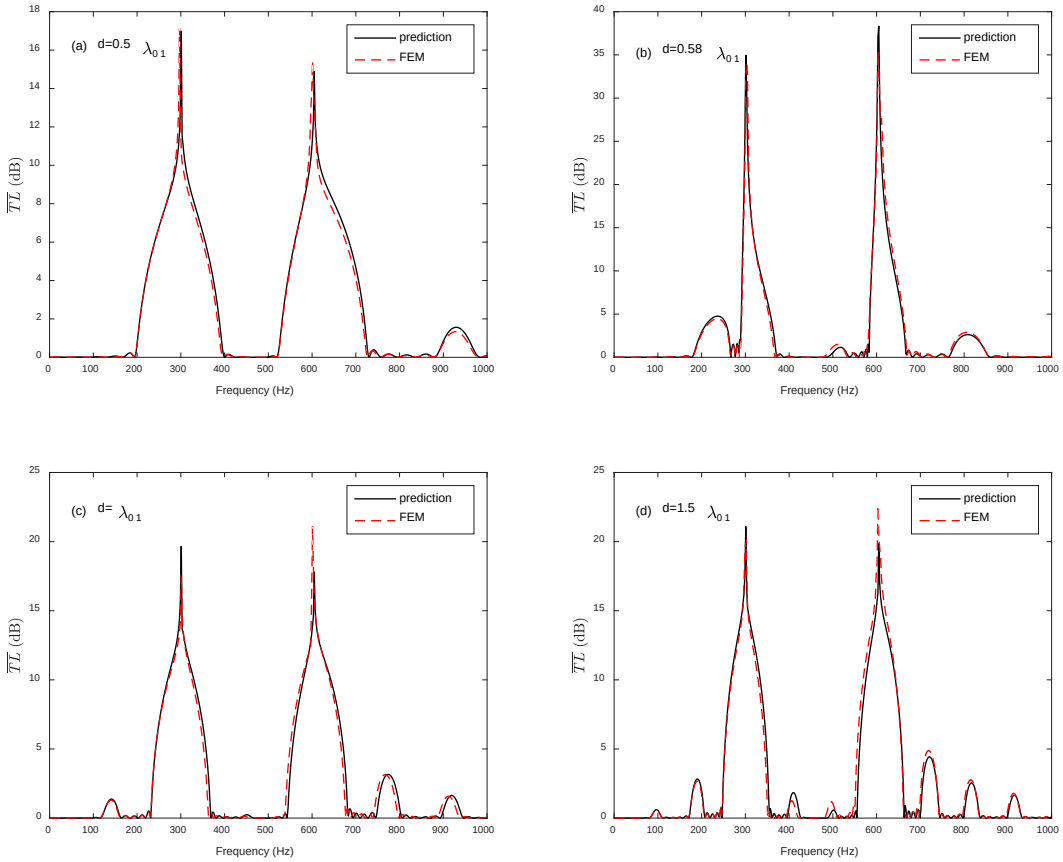

Fig. 8 The average transmission loss of the periodic dual HR system in respect of different periodic distances (solid lines represent the theoretical predictions, and dashed lines represent the FEM simulation results)

5. Conclusion

This paper focuses on the hybrid noise control by using a periodic dual HR array, and presents theoretical and numerical studies of a periodic dual HR system. The dual HR which consists of two HRs connected in series (neck-cavity-neck-cavity) leads to two resonance frequencies. The geometries of the dual HR are significant small compared with the wavelengths. Hence, the lumped parameter theory is employed to approximate the dual HR as an equivalent two degrees of freedom mechanical system. The resonance frequencies and transmission loss of a dual HR have been derived. Aiming at broader noise attenuation bands for hybrid noise control at low frequencies, a duct with an array of dual HRs distributed periodically is investigated. In the interest of low frequencies, the frequency range considered in this paper is well below the duct's cutoff frequency. It is therefore that only planar wave is allowed to propagate in the duct. Owing to the coupling of Bragg reflection and dual HR's resonances, a periodic dual array can provide much broader noise attenuation bands at the designed resonance frequencies of the dual HR. In order to make the first and second Bragg reflection coincide with two resonance frequencies of the dual HR respectively, the periodic distance is set to be $d = \lambda_{01}/2 = \lambda_{02}$. Therefore, two broader noise attenuation bands at the dual HR's resonances can be achieved. The proposed periodic dual HR array can be used in practical engineering work to reduce hybrid noise at low frequencies.

Acknowledgements

The work described in this paper was fully supported by a grant from the Research Grants Council of the Hong Kong Special Administrative Region, China (Project No. PolyU 152116/14E).

References

[1] Harris M. Handbook of noise control. New York: McGraaw-Hill; 1979.

[2] Fahy F. Foundations of engineering acoustics. Amsterdam: Elsevier; 2001.

[3] Sohn CH, Park JH. A comparative study on acoustic damping induced by half-wave, quater-wave, and Helmholtz resonator. Aerosp Sci Technol 2011; 15(8):606-614.

[4] Mak CM, Yang J. A prediction method for aerodynamic sound produced by closely spaced elements in air ducts. J Sound Vib 2000;229(3):743-753.

[5] Kreider JF. Handbook of heating ventilation and air conditioning. Boca Raton: CRC Press; 2000.

[6] Mak CM, Liu YP. The effect of sound on office productivity. Build Serv Eng Res T 2012; 33(3):339-345.

[7] Namba S, Kuwano S. Okamoto T. Sleep disturbance caused by meaningful sounds and effect of background noise. J Vib Acoust 2004;277:445-452.

[8] Toyoda M, Sakagami K, Okano M, Okuzono T, Toyoda E. Improved sound absorption performance of three-dimensional MPP space sound absorbers by filling with porous materials. Appl Acoust 2017;116:311-316.

[9] Peak KS, Rathi KL. A finite element analysis of the convected acoustic wave motion in dissipative silencers. J Sound Vib 1995;184(3):529-45.

[10] Sakagami K, Fukutani Y, Yairi M, Morimoto M. A theoretical study on the effect of a permeable membrane in the air cavity of a double-leaf microperforated panel space sound absorber. Appl Acoust 2014;79:104-109.

[11] Ingard U. On the theory and design of acoustic resonators. J Acoust Sco Am 1953;25: 1037-1061.

[12] Cai C, Mak CM, Shi X. An extended neck versus a spiral neck of the Helmholtz resonator. Appl Acoust 2017;115:74-80.

[13] Cai C, Mak CM. Noise attenuation capacity of a Helmholtz resonator. Adv Eng Softw 2018;116:60-66.

[14] Griffin S, Lane SA, Huybrechts S. Coupled Helmholtz resonators for acoustic attenuation. J Vib Acoust 2001;123:11-17.

[15] Xu MB, Selamet A, Kim H. Dual Helmholtz resonator. Appl Acoust 2010;71:822-829.

[16] Guan C, Jiao Z. Modeling and optimal design of 3 degrees of freedom Helmholtz resonator in Hydraulic system. Chinese J Aeronaut 2012;25:776-783.

[17] Park SH. Acoustic properties of micro-perforated panel absorbers backed by Helmholtz resonators for the improvement of low-frequency sound absorption. J Sound Vib 2013;332:4895-4911.

[18] Bradley CE. Time harmonic acoustic Bloch wave propagation in periodic waveguides. Part I. Theory. J Acoust Soc Am 1994;96:1844-1953.

[19] Bradley CE. Time harmonic acoustic Bloch wave propagation in periodic waveguides. Part I. Experiment. J Acoust Soc Am 1994;96:1854-1962.

[20] Sugimoto A, Horioka T. Dispersion characteristics of sound waves in a tunnel with an array of Helmholtz resonators. J Acoust Soc Am 1995;97(3):1446-1459.

[21] Cai C, Mak CM. Noise control zone for a periodic ducted Helmholtz resonator system. J Acoust Soc Am 2016;140(6):EL471-EL477.

[22] Cai C, Mak CM, Wang X. Noise attenuation performance improvement by adding Helmholtz resonators on the periodic ducted Helmholtz resonator systems. Appl Acoust 2017;122:8-15.

[23] COMSOL. Acoustic Module User's Guide. Version 5.1;2015.

Figure captions

Fig. 1 Mechanical analogy of a dual Helmholtz resonator

Fig. 2 Schematic diagram of a periodic dual HR system

Fig. 3 Comparison of the theoretical predictions and FEM simulation results (solid line represents the theoretical predictions, and dashed line represents the FEM simulation results)

Fig. 4 Configuration of the periodic dual HR system consisting of six dual HRs

Fig. 5 Noise attenuation bands of the periodic dual HR system due to Bragg reflection and dual HR's resonances separately

Fig. 6 Noise attenuation bands of the periodic dual HR system due to the coupling of Bragg reflection and dual HR's resonances

Fig. 7 Noise attenuation bands of the periodic dual array system with and without coupling effects

Fig. 8 The average transmission loss of the periodic dual HR system in respect of different periodic distances (solid lines represent the theoretical predictions, and dashed lines represent the FEM simulation results)